Electrocardiogram Signal Classification for Heart Disease Identification

Minh Phung
Department of Electronics, Ho Chi Minh City University of Technology, Ho Chi Minh City, Vietnam | Vietnam National University Ho Chi Minh City, Ho Chi Minh City, Vietnam
minh.phung2002sn@hcmut.edu.vn

Hieu Nguyen
Department of Electronics, Ho Chi Minh City University of Technology, Ho Chi Minh City, Vietnam | Vietnam National University Ho Chi Minh City, Ho Chi Minh City, Vietnam
hieunt@hcmut.edu.vn (corresponding author)

Linh Tran
Department of Electronics, Ho Chi Minh City University of Technology, Ho Chi Minh City, Vietnam | Vietnam National University Ho Chi Minh City, Ho Chi Minh City, Vietnam
linhtran@hcmut.edu.vn

Received: 7 March 2025 | Revised: 2 April 2025 and 14 April 2025 | Accepted: 19 April 2025

 DOI: https://doi.org/10.48084/etasr.9027

ABSTRACT

Cardiovascular diseases are among the leading causes of death worldwide, and diagnosing them based on Electrocardiogram (ECG) signals traditionally requires highly experienced doctors. However, with advancements in artificial intelligence, machine learning models have been increasingly used to assist in diagnosing cardiovascular diseases without the need for direct doctor evaluation. Identifying heart disease through ECG signals presents several challenges, such as measurement noise and the continuous nature of ECG data. In this paper, we propose a method to address these challenges and achieve high diagnostic efficiency. To evaluate our approach, we utilize the MIT-BIH Arrhythmia Database. Experimental results demonstrate that our algorithm can classify ECG signals into five categories with significantly higher accuracy compared to previous methods.

Keywords-heart disease identification; electrocardiogram signal; classification

I. INTRODUCTION

According to the World Health Organization (WHO), cardiovascular diseases are among the leading causes of death worldwide [1]. Traditionally, doctors diagnose cardiovascular conditions by analyzing electrocardiogram (ECG) signals, with accurate diagnosis requiring cardiologists with extensive experience in the field. However, in many developing countries, the number of trained specialists is insufficient relative to patient demand, resulting in an overload of hospital resources.

With technological advancements in recent years, machine learning models have been increasingly employed to diagnose cardiovascular diseases remotely using ECG signals, thereby reducing the dependence on cardiologists. Consequently, numerous studies have focused on developing machine learning approaches for ECG-based cardiovascular disease diagnosis.

When acquiring ECG signals, various types of data noise may be introduced, such as from patient movement, poor electrode-skin contact, or power line interference. Therefore, noise removal is a critical first step in ECG signal processing. As a result, authors in [2-4] proposed using cascaded low-pass and high-pass filters to create a band-pass filter. However, given that ECG signals are non-stationary, time-frequency domain techniques are generally more appropriate than purely frequency-based methods [5, 6]. Authors in [7] showed that the wavelet transform is one of the most suitable and effective methods in processing non-stationary signals.

An ECG signal comprises P, QRS, and T waves within each cardiac cycle [8]. Following acquisition, the dataset typically consists of continuous ECG recordings that must be segmented into individual beats. This segmentation requires accurate detection of the R peak locations. Authors in [9] proposed a Rapid-Ramp Effective Algorithm for R peak detection based on slope analysis between adjacent samples. However, this method was validated on only two records and suffers from high computational complexity. In [10], a hybrid approach combining Empirical Mode Decomposition and the Hilbert Transform was proposed for R peak detection, but it is computationally intensive. In [11], Coiflet wavelets were used with Discrete Wavelet Transform (DWT) for removing noise the data. In this method, the negative R peaks cases are handled by squaring the signal, but this leads to an increase in the number of peaks, reducing the moving averages algorithm accuracy. Authors in [11-15] employed the Two Event-Related Moving Averages (TERMA) method to detect ECG peaks, but this approach does not effectively handle negative R peaks and struggles when T peaks are nearly equal to or higher than R peaks. Authors in [16] proposed an algorithm that mirrors negative peaks based on slope, addressing negative R peaks, but the method exhibited low accuracy due to a high rate of false positives.

Each ECG waveform pattern corresponds to a specific type of cardiovascular disease. Once segmented, individual ECG beats can be used as inputs for machine learning algorithms aimed at classifying various cardiovascular conditions. Authors in [17-22] proposed classification methods capable of distinguishing five classes: Normal Beat (N), Supraventricular Ectopic Beat (S), Ventricular Ectopic Beat (V), Fusion Beat (F), and Unknown Beat (Q), according to the American Association for the Advancement of Medical Instrumentation (AAMI) standards [23]. While this grouping increases the number of samples per class, it limits the ability to identify specific diseases precisely. Alternatively, authors in [13] proposed classification approaches using Support Vector Machine (SVM) and Multi-Layer Perceptron (MLP) algorithms, while [24] and [25] trained Convolutional Neural Networks (CNNs) for ECG classification. These methods focus on five distinct classes: Normal Beat (Normal), Premature Atrial Beat (PAC), Premature Ventricular Contraction (PVC), Left Bundle Branch Block Beat (LBBB), and Right Bundle Branch Block Beat (RBBB). This categorization allows for more precise identification of specific cardiovascular diseases represented by the ECG signals.

In this study, we first apply DWT to eliminate high-frequency noise and baseline drift. We then propose a novel algorithm for R peak detection that effectively handles negative R peaks, distinguishes between R and T peaks even when their amplitudes are comparable, and does not depend on the absolute value of the R peak. Finally, we introduce a CNN-based classification model to categorize ECG signals into five classes: Normal, PAC, PVC, LBBB, and RBBB. Our approach is evaluated using datasets from the highly reliable MIT-BIH Arrhythmia Database [26], publicly available at [27].

II. PRELIMINARIES

A. Discrete Wavelet Transform (DWT)

Wavelet transformation is one of the most suitable and effective methods in processing non-stationary signals [7]. In this transformation, two important parameters are the scale a and the position b, using the wavelet function $\Psi(t)$. When the scale parameter a is restricted to powers of two ($a = 2^j$ the wavelet is called a dyadic wavelet [28]. An efficient way to implement this scheme using filters was developed in 1988 by the authors in [29] called DWT. Two coefficient groups are defined: the approximation coefficient cA_x and the detail coefficient cD_x. cA_x represents the low-frequency components of the signal, while cD_x represents the high-frequency components. The decomposition process can be iterated, with each approximation further decomposed into lower-resolution components, forming a decomposition tree as shown in Figure 1. At each level, downsampling is applied, reducing the number of signal elements. To reconstruct the original signal, the Inverse Discrete Wavelet Transform (IDWT) is used.

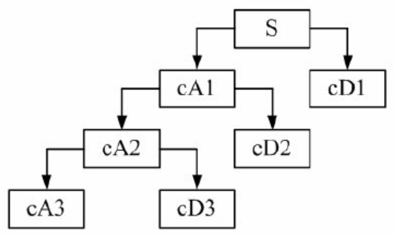

Fig. 1. Wavelet decomposition tree.

Each decomposition level j is related to a certain frequency range [30]. Thus, the decomposition level can be calculated depending on the needed pseudo-frequency by using (1):

$$F_a = \frac{F_c}{a\Delta} \quad (1)$$

where:

- F_a is a pseudo-frequency related to a certain decomposition level j.
- F_c is the central frequency of the wavelet function.
- $a = 2^j$ is the scale parameter.
- Δ is the sampling period.

B. Convolutional Neural Network (CNN)

CNN is widely used in tasks like image recognition and video analysis. Authors in [31] compared the accuracy of various pre-trained CNNs for sound signal classification and found VGGish and YAMNet to be the most suitable. VGGish adapts the Visual Geometry Group (VGG) architecture for audio classification, while YAMNet, based on the MobileNet architecture, is designed to recognize environmental sounds. Both models apply CNN principles to audio data, enabling sound classification and event detection.

Since ECG signals are non-stationary, similar to audio signals, these architectures have strong potential for effective ECG analysis, and are used in this study.

1) VGGish Neural Network

VGGish has 24 layers, including the input layer, as shown in Figure 2(a). It comprises two blocks of three layers (a convolutional layer, a ReLU activation layer, and a max-pooling layer), two blocks of five layers (two convolutional layers, two ReLU activation layers, and one max-pooling layer), and one block of six layers (three fully connected layers and three ReLU activation layers). VGGish contains nine layers with learnable weights (six convolutional layers and three fully connected layers) totaling 72,141,184 learnable parameters.

2) YAMNet neural network

YAMNet has 86 layers, including the input layer, as shown in Figure 2(b). A block of six layers (a convolutional layer, a batch normalization layer, a ReLU activation layer, a grouped convolutional layer, a batch normalization layer, and a ReLU activation layer) is repeated 13 times. Grouped convolutional layers are employed to reduce computational resource consumption during training. YAMNet has 28 layers with learnable weights, including 27 convolutional layers and one fully connected layer, totaling 3,751,369 learnable parameters.

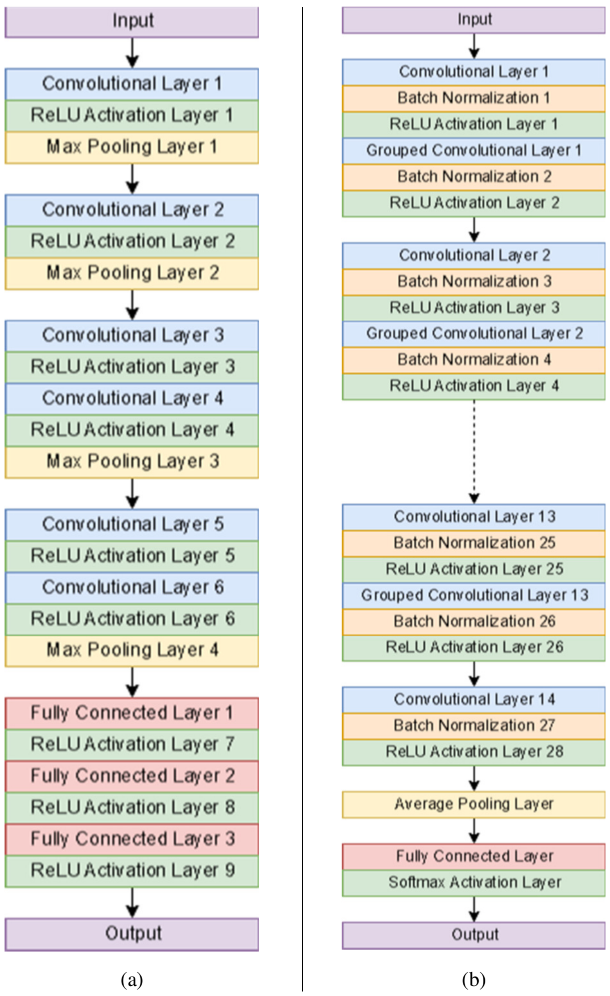

Fig. 2. (a) VGGish structure, (b) YAMNet structure.

III. PROPOSED METHOD

A. Denoising using DWT

The method proposed in [32] was applied in [33], which concluded that the most suitable wavelet function for ECG signals is Daubechies 4, with a central frequency of 0.7 Hz. The proposed method was tested on the MIT-BIH dataset [25], which has a sampling frequency (F_s) of 360 Hz. Using equation (1), the pseudo-frequency for each decomposition level can be calculated, as shown in Table I.

Noise in ECG signals includes high-frequency noise (≥128 Hz) and baseline drift (0 - 1 Hz). Therefore, an eight-level decomposition is applied, and only the detail coefficients from levels 2 to 7 are used for signal reconstruction.

TABLE I. PSEUDO-FREQUENCY F_a FOR EACH DECOMPOSITION LEVEL j

j	1	2	3	4	5	6	7	8	9
$a = 2^j$	2^1	2^2	2^3	2^4	2^5	2^6	2^7	2^8	2^8
F_a (Hz)	128	64	32	16	8	4	2	1	0.5

B. R Peaks Detection Algorithm

The proposed R peaks detection algorithm includes 3 steps as shown in Figure 3:

- Mirroring the negative signal selectively.
- Detecting the set of potential R peaks.
- Detecting correct R peaks from the previous set.

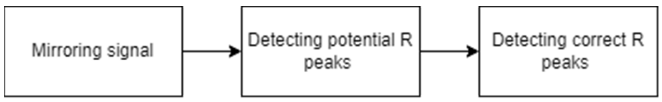

Fig. 3. R peaks detection algorithm's block diagram.

The algorithm was implemented on the MATLAB 2023 tool.

1) Mirroring Signal Algorithm

The proposed method mirrors only those negative data points that have at least one neighboring negative data point within a range of $\Delta t(s)$ before and after the current point, with absolute values not exceeding 1.5 times that of the current point.

Pseudocode of algorithm 1: Mirroring signal algorithm:

```
Fs ← 360,  Δt ← 0.1
for each point (ECG[i]) of ECG signal do:
  if ECG[i] ≥ 0
    Continue process next data point
  end if

  for each point ECG[j] do
where j in range [i − Δt * Fs, i]
    if ECG[j] < 0 and |ECG[j]| ≤ 1.5 * |ECG[i]|
      Point ECG[i] satisfy condition 1.
      Break for loop.
    end if
  end for
  for each point ECG[j]  do
where j in range [i, i + Δt * Fs]
    if ECG[j] < 0 and |ECG[j]| ≤ 1.5 * |ECG[i]|
```

```
    Point ECG[i] satisfy condition 2.
    Break for loop.
  end if
end for

if point ECG[i] satisfy both conditions
  Mirroring point ECG[i].
end if
end for
```

Figure 4 illustrates the result of the mirroring algorithm applied to record 200 of the MIT-BIH dataset, with the red line representing the original signal and the blue line shows the output of the proposed algorithm. It is shown that only high-slope peaks were mirrored.

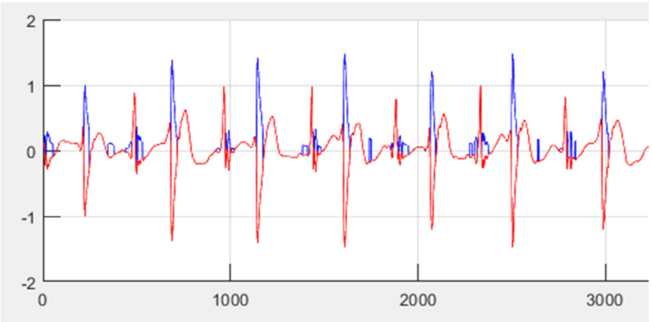

Fig. 4. Result of the mirroring algorithm when applied to record 200.

2) Potential R Peaks Detection

Similar to the TERMA algorithm in [12], we use two moving average methods to find out the Blocks of Interest (BOI). The potential R peaks are the largest data points within each BOI. We choose the W_{cycle} equal to the ECG signal period 0.8 sec then $W_{cycle} = 0.8 \cdot F_s \approx 300$. Because the QRS complex is lasted for 0.3 s, so we choose $W_{event} = 0.3 \cdot F_s \approx 108$.

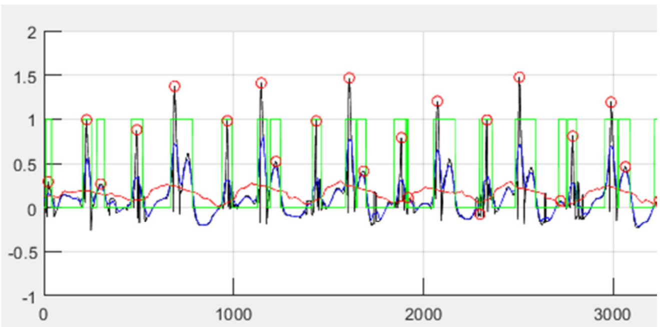

Fig. 5. Result of potential R peaks detection algorithm.

Figure 5 illustrates the result of the potential R peaks detection algorithm when applied to record 200 of the MIT-BIH dataset, after applying the mirroring signal algorithm. The lines in Figure 5 are described as follows:

- The black line is the mirrored signal.
- The red line is the cycle moving average line.
- The blue line is the event moving average line.
- The green line illustrates the BOI.
- The red circles illustrate the potential R peaks.

3) Correct R Peaks Detection Algorithm

In the proposed method, two threshold values are used:the amplitude threshold th_{amp} and the interval threshold th_{itv}.

$$th_{amp} = k_{amp} \cdot r_{avr_{amp}} \quad (2)$$

$$th_{itv} = k_{itv} \cdot r_{avr_{itv}} \quad (3)$$

where:

- k_{amp} is a coefficient ranging between 0 to 1.
- $r_{avr_{amp}}$ is the average amplitude of the correct R peaks; if fewer than 4 correct R peaks are found, it is set to the maximum value of the ECG signal.
- k_{itv} is a coefficient ranging between 0 to 1.
- $r_{avr_{itv}}$ is the average of the interval of pairs of 2 adjacent correct R peaks. If the number of correct R peaks is less than 4, $r_{avr_{itv}}$ is equal to the ECG period multiplied by F_s.

The pseudocode for the correct R peak detection algorithm is described below, where $pot\_r\_loc[i]$ is the location of the i^{th} potential R peak and $mir\_ecg[x]$ is the amplitude of the mirrored ECG signal at position x.

Pseudocode of algorithm 2: Detecting correct R peaks algorithm:

```
Fs ← 360,  Δt ← 0.1
for each potential R peak pot_r_loc[i] and
number of potential R peak ≥ 2 do:
  Update th_amp and th_itv.

  if  mir_ecg[pot_r_loc[i]] < th_amp
    Remove current potential R peak.
    Continue process next potential R
peak.
  end if

  if pot_r_loc[i] − pot_r_loc[i − 1] > th_itv
    i − 1 is the correct R peak.
  else
   if mir_ecg[pot_r_loc[i]] ≥ mir_ecg[pot_r_loc[i −
1]]
     Remove i - 1 potential R peak.
   else
     Remove i potential R peak.
   end if
  end if
end for
```

Figure 6 shows the result of the correct R peak detection algorithm when applied to record 200 of the MIT-BIH dataset. The blue line is the mirrored ECG signal, and the red circles are correct R peaks.

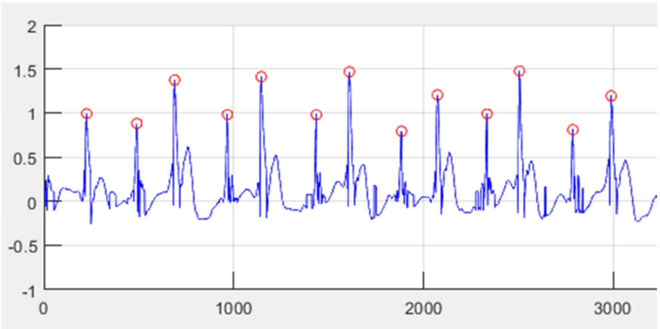

Fig. 6. Result of detecting correct R peaks algorithm.

C. *ECG Signal Classification*

For testing the classification algorithm, we use the data from 43 records of the MIT-BIH dataset. Each record undergoes the filtering and R peak detection algorithms. Since R peaks are considered the center of each heartbeat, for each beat, a segment of 150 samples before and 149 samples after the R peak is extracted, resulting in a 300-point signal per beat. The classification algorithm categorizes each beat into five classes: Normal, PAC, PVC, LBBB, and RBBB. Data from the MIT-BIH dataset is divided into 70% for training, 15% for validation, and 15% for testing.

IV. RESULTS AND DISCUSSION

The results of the training process on YAMNet and VGGish are shown in Figure 7, with very similar resulting validation accuracies of 99.40% and 99.32%, respectively, as shown in Table II.

TABLE II. TESTING RESULTS OF THE TRANSFER LEARNING METHOD

CNN	YAMNet	VGGish
Validation Accuracy (%)	99.41	99.32

The training results of the proposed algorithm are shown in Table III. The table shows the number of predicted R peaks using the algorithm (column 2) and the number of annotated R peaks by the dataset (column 3). In addition, we use the metrics: True Positive (TP), False Negative (FN), False Positive (FP), Precision (P), and Recall (R). We mainly focus on Precision representing the ratio of correctly detected peaks to total detected peaks, and Recall representing the ratio of correctly detected peaks to total peaks of samples. In most cases, two parameters are higher than 0.98 except in some special cases: No. 5, 14, 20, 23, 25, 36. We analyze the results of No. 14 in Figure 8. The figure shows a section with many errors in dataset No. 14. The green circle is the correct position of peak R, and the red circle is the result of the algorithm. The reason is that the negative peak next to peak R has an absolute value larger than peak R. After performing the Mirroring Signal step, that peak is always higher than the actual peak R, and the Peak Detection algorithm chooses the highest peak leading to the wrong detection. We analyze another result in Figure 9: No. 25. The illustration shows that the full ECG signal of this sample has many noisy parts. This part is the reason why the Peak Detection algorithm is wrong. Zoom in on these parts and we get the result as shown in Figure 10. The noise in this part of the signal is so large compared with the main signal that it changes the shape of the ECG signal. That is the reason why the Peak Detection algorithm returns the wrong result.

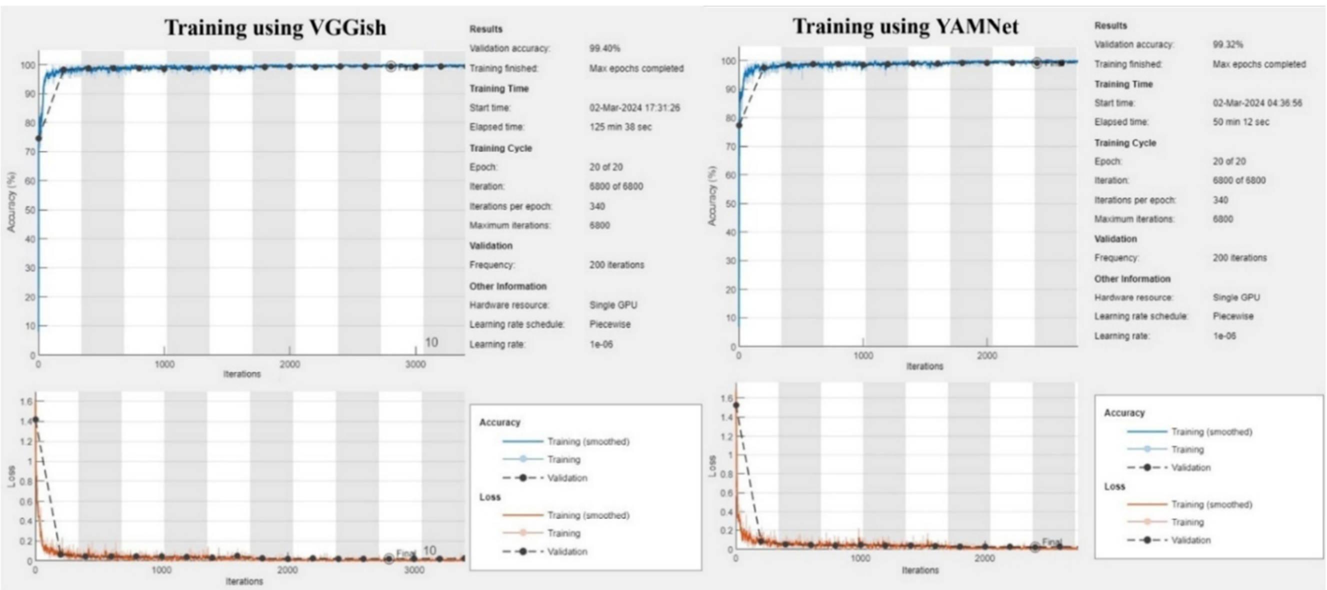

Fig. 7. Result of the training process on YAMNet and VGGish.

TABLE III. RESULT OF THE PROPOSED R PEAKS DETECTION ALGORITHM

No.	File	R peaks (P)	R peaks (A)	TP	FN	FP	P	R
1	100	2272	2274	2272	2	0	1	0.9991
2	101	1864	1874	1863	11	1	0.9995	0.9941
3	103	2079	2091	2079	12	0	1	0.9943
4	105	2573	2691	2497	194	76	0.9705	0.9279
5	106	1557	2098	1552	546	5	0.9968	0.7398
6	108	1749	1824	1631	193	118	0.9325	0.8942
7	109	2532	2535	2494	41	38	0.985	0.9838
8	111	1920	2133	1917	216	3	0.9984	0.8987
9	112	2538	2550	2538	12	0	1	0.9953
10	113	1793	1796	1793	3	0	1	0.9983
11	115	1950	1962	1950	12	0	1	0.9939
12	116	1964	2421	1960	461	4	0.998	0.8096
13	117	1534	1539	1534	5	0	1	0.9968
14	118	2277	2301	2142	159	135	0.9407	0.9309
15	119	1986	2094	1986	108	0	1	0.9484
16	121	1859	1876	1857	19	2	0.9989	0.9899
17	122	2475	2479	2475	4	0	1	0.9984
18	123	1517	1519	1517	2	0	1	0.9987
19	124	1611	1634	1602	32	9	0.9944	0.9804
20	200	2105	2792	2088	704	17	0.9919	0.7479
21	201	1780	2039	1747	292	33	0.9815	0.8568
22	202	2113	2146	2111	35	2	0.9991	0.9837
23	203	2152	3108	2119	989	33	0.9847	0.6818
24	205	2630	2672	2630	42	0	1	0.9843
25	207	1996	2385	1898	487	98	0.9509	0.7958
26	208	2910	3040	2884	156	26	0.9911	0.9487
27	209	2996	3052	2996	56	0	1	0.9817
28	210	2520	2685	2519	166	1	0.9996	0.9382
29	212	2744	2763	2744	19	0	1.0000	0.9931
30	213	3235	3294	3204	90	31	0.9904	0.9727
31	214	2250	2297	2173	124	77	0.9658	0.9460
32	215	3345	3400	3345	55	0	1.0000	0.9838
33	219	2146	2312	2146	166	0	1.0000	0.9282
34	220	2047	2068	2047	21	0	1.0000	0.9898
35	221	2416	2462	2412	50	4	0.9983	0.9797
36	222	2078	2634	2078	556	0	1.0000	0.7889
37	223	2134	2643	2132	511	2	0.9991	0.8067
38	228	2037	2141	1995	146	42	0.9794	0.9318
39	230	2252	2466	2252	214	0	1.0000	0.9132
40	231	1566	2011	1566	445	0	1.0000	0.7787
41	232	1772	1816	1771	45	1	0.9994	0.9752
42	233	3063	3152	2960	192	103	0.9664	0.9391
43	234	2748	2764	2748	16	0	1.0000	0.9942
Total		95085	101833	94224	7609	861	0.9909	0.9253

Second, we apply YAMNet and VGGish CNN models to classify five classes of ECG signals. The classification results for each class are presented in Table IV, Table V, and Table VI, respectively. Additionally, we compare the performance of the proposed CNN method with other methods across the five classes. To evaluate the performance, three metrics are used: Precsion, Recall and F1 Score. F1 Score can be understood as the average value between Precision and Recall. The larger these parameters, the better the algorithm's accuracy. Our algorithm focuses on correctly classifying the ECG into 5 classes, so we need these parameters in all classes as significant as possible. From three tables, our algorithm (No 4 and No 5) all have values greater than 91% in 5 classes. Compared with CNN in [24], these values are not good in PAC classes. Compared with SVM in [13], although it has 100 in PAC, PVC, and LBBB classes, these values in Normal and RBBB classes are bad. More specifically, the VGGish has the best score (all greater than 98) in 4 classes: Normal, PVC, RBBB, and LBBB. Meanwhile, YAMNet has worse results in Normal class, better results in PAC class, and almost equal results in the three remaining classes.

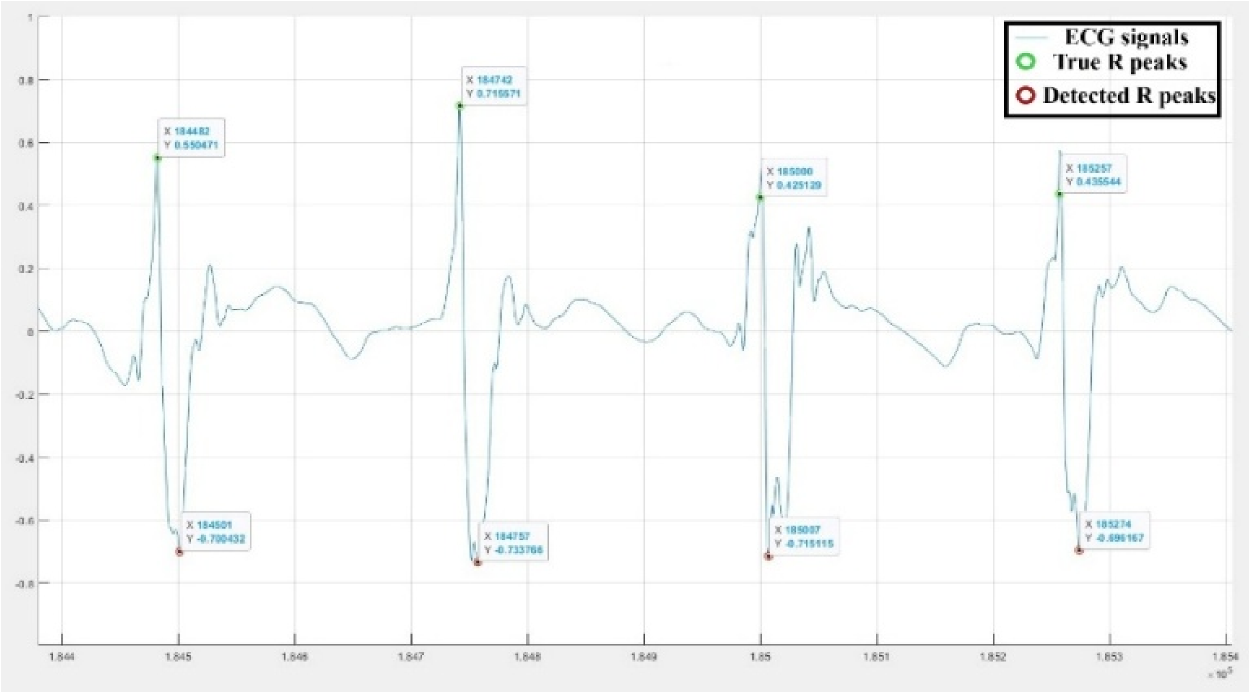

Fig. 8. Result of No. 14.

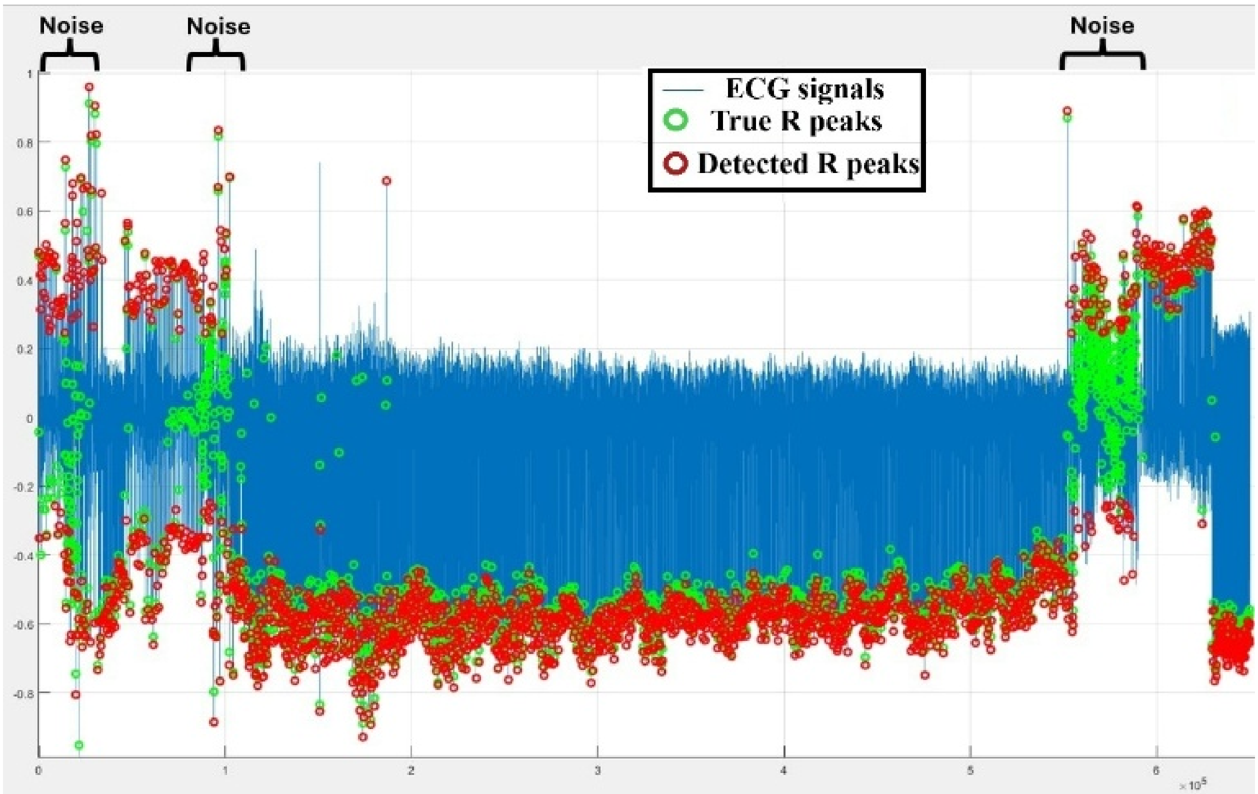

Fig. 9. Result of No. 25.

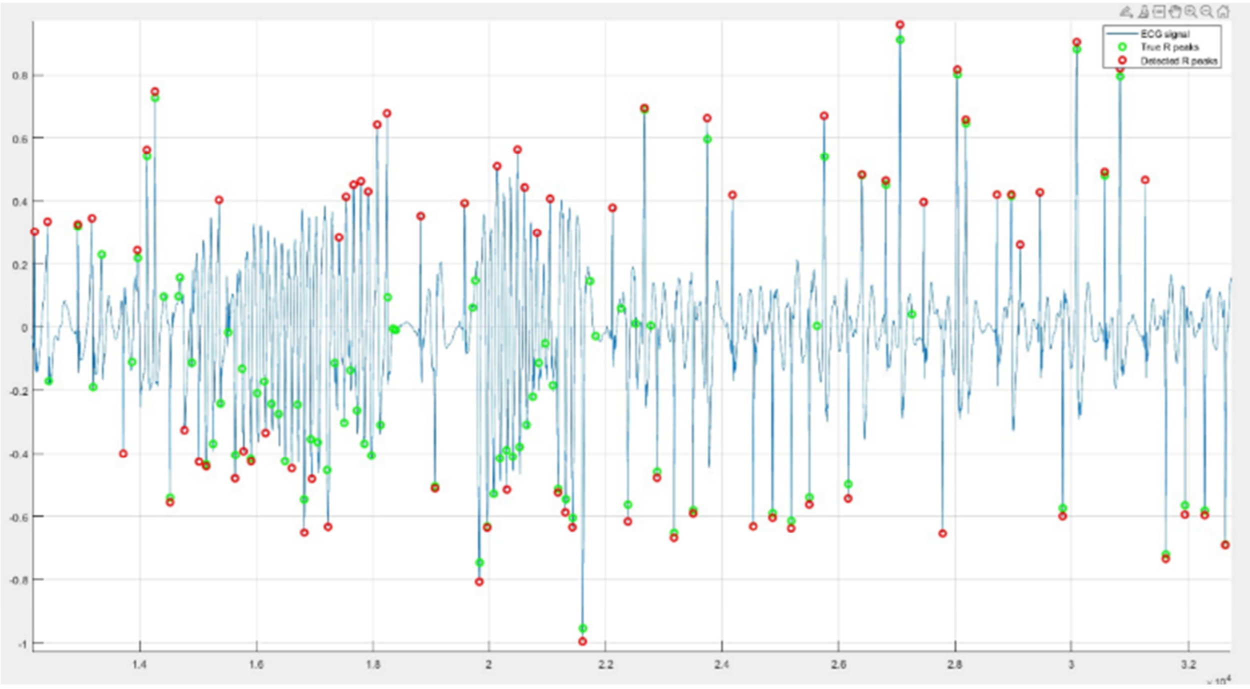

Fig. 10. Detailed result of the noisy part in sample No. 25.

TABLE IV. COMPARISON IN NORMAL CLASS (%)

No	Method	Normal		
		Precision	Recall	F1-score
1	SVM [13]	52.4	98.5	68.4
2	MLP [13]	81.5	74.6	77.9
3	CNN [24]	98.6	98.7	98.6
4	YAMNet	94.102	92.368	93.227
5	VGGish	99.515	99.798	99.657

TABLE V. COMPARISON IN PAC, PVC CLASS (%)

No	Method	PAC			PVC		
		Precision	Recall	F1-score	Precision	Recall	F1-score
1	SVM [13]	100	100	100	100	100	100
2	MLP [13]	84.5	74.8	79.3	100	84.4	91.6
3	CNN [24]	96.2	81.9	88.5	98.4	93.6	95.9
4	YAMNet	99.834	99.421	99.627	99.551	99.752	99.652
5	VGGish	96.111	91.053	93.514	98.828	98.348	98.587

TABLE VI. COMPARISON IN RBBB, LBBB CLASS (%)

No	Method	RBBB			LBBB		
		Precision	Recall	F1-score	Precision	Recall	F1-score
1	SVM [13]	81.8	7	13	100	100	100
2	MLP [13]	74.9	74.6	74.8	68.1	87.1	76.5
3	CNN [24]	88.4	96	92	97.8	99.1	98.4
4	YAMNet	99.54	99.357	99.448	98.727	97.959	98.341
5	VGGish	99.631	99.265	99.448	99.752	99.587	99.669

To have better comments, we evaluate the resource consumption of two architectures on two devices. The results are shown in Table VII. YAMNet consumes fewer resources and has less running time compared with VGGish. In short, YAMNet is suitable with low resource requirements applications, but it trades off with less accuracy. In contrast, VGGish is suitable for applications requiring high precision and has a lot of hardware resources.

TABLE VII. COMPARE RESOURCE CONSUMPTION

CNN		YAMNet	VGGish
Number of learnable parameters (weights and biases)		3200592	71636749
Parameter memory (MB)		12.20928955	273.2725105
Floating point operations (FLOPs)		137396224	1726905378
Inference time (s)	**Device 1:** Window 10, Processor Intel(R) Core(TM) i7-6700HQ CPU 2.60GHz, RAM 16GB	0.007409	0.104775
	Device 2: Window 11, Processor 12th Gen Intel(R) Core(TM) i5-12500H 2.50 GHz, RAM 16GB	0.006622	0.004856

V. CONCLUSION

This work proposes a new technique, which employs an innovative deep learning structure, to classify ECG signals. Our research begins with an algorithm designed to detect R peaks, followed by a CNN-based method that utilizes the YAMNet and VGGish models to classify ECG signals. The main novelty of this study is in formulating an improved algorithm for detecting R peaks. This method combines time-frequency domain features obtained from a signal with sophisticated attention-based neural architecture. It enhances the ability to separate noise processes masking variations of ECG signals which has been a considerable problem in the literature.

Unlike most previous approaches where classification is done using a CNN or SVM and MLP, our technique is based on a more sophisticated and flexible feature extraction design. While CNN-based approaches are good at spatial dependency and the others at the emphasis of sequential patterns, our model uses both. Furthermore, it has an attention-based feature that focuses on the most important signal attributes. These improvements facilitate more effective and accurate classification of ECG signals. The experimental results in Section IV show that our algorithm outperforms other algorithms.

Our algorithm is expected to work with not only normal people but also people who have cardiovascular diseases. However, our algorithm does not detect other kinds of cardiovascular diseases. In future work, we intend to develop another algorithm that maintains accuracy and costs less resources. We aim to develop algorithms that can be embedded in microprocessors to be used in handheld devices.

ACKNOWLEDGMENT

We acknowledge Ho Chi Minh University of Technology (HCMUT), VNU-HCM for supporting this study.

REFERENCES

[1] G. R. Dagenais *et al.*, "Variations in common diseases, hospital admissions, and deaths in middle-aged adults in 21 countries from five continents (PURE): a prospective cohort study," *The Lancet*, vol. 395, no. 10226, pp. 785–794, Mar. 2020, https://doi.org/10.1016/S0140-6736(19)32007-0.

[2] H. C. Chen and S. W. Chen, "A moving average based filtering system with its application to real-time QRS detection," in *Computers in Cardiology, 2003*, Thessaloniki Chalkidiki, Greece, 2003, pp. 585–588, https://doi.org/10.1109/CIC.2003.1291223.

[3] J. Pan and W. J. Tompkins, "A Real-Time QRS Detection Algorithm," *IEEE Transactions on Biomedical Engineering*, vol. BME-32, no. 3, pp. 230–236, Mar. 1985, https://doi.org/10.1109/TBME.1985.325532.

[4] L. Sathyapriya, L. Murali, and T. Manigandan, "Analysis and detection R-peak detection using Modified Pan-Tompkins algorithm," in *2014 IEEE International Conference on Advanced Communications, Control and Computing Technologies*, Ramanathapuram, India, May 2014, pp. 483–487, https://doi.org/10.1109/ICACCCT.2014.7019490.

[5] Y. Wang, W. Wu, Q. Zhu, and G. She, "Discrete Wavelet Transfom for Nonstationary Signal Processing," in *Discrete Wavelet Transforms - Theory and Applications*, J. T. Olkkonen, Ed. InTech, 2011.

[6] G. Tzanetakis, G. Essl, and P. Cook, "Audio analysis using the discrete wavelet transform," in *Proceedings of the WSES International Conference Acoustics and Music: Theory and Applications (AMTA 2001)*, Jan. 2001, pp. 318-323.

[7] M. Alam, Md. I. Islam, and M. R. Amin, "Performance Comparison of STFT, WT, LMS and RLS Adaptive Algorithms in Denoising of Speech Signal," *International Journal of Engineering and Technology*, vol. 3, no. 3, pp. 235–238, 2011, https://doi.org/10.7763/IJET.2011.V3.230.

[8] J. Malmivuo and R. Plonsey, *BioelectromagnetismPrinciples and Applications of Bioelectric and Biomagnetic Fields*. Oxford University Press, 1995.

[9] O. Adeluyi and J.A. Lee, "R-reader: A lightweight algorithm for rapid detection of ecg signal r-peaks," in *2011 2nd International Conference on Engineering and Industries (ICEI)*, Seogwipo, South Korea, 2011, pp. 1-5.

[10] R. Mabrouki, B. Khaddoumi, and M. Sayadi, "R peak detection in electrocardiogram signal based on a combination between empirical mode decomposition and Hilbert transform," in *2014 1st International Conference on Advanced Technologies for Signal and Image Processing (ATSIP)*, Sousse, Tunisia, Mar. 2014, pp. 183–187, https://doi.org/10.1109/ATSIP.2014.6834603.

[11] M. Elgendi, M. Jonkman, and F. De Boer, "R wave detection using Coiflets wavelets," in *2009 IEEE 35th Annual Northeast Bioengineering Conference*, Cambridge, MA, USA, Apr. 2009, pp. 1–2, https://doi.org/10.1109/NEBC.2009.4967756.

[12] M. Elgendi, "TERMA Framework for Biomedical Signal Analysis: An Economic-Inspired Approach," *Biosensors*, vol. 6, no. 4, Nov. 2016, Art. no. 55, https://doi.org/10.3390/bios6040055.

[13] S. Aziz, S. Ahmed, and M.S. Alouini, "ECG-based machine-learning algorithms for heartbeat classification," *Scientific Reports*, vol. 11, no. 1, Sep. 2021, Art. no. 18738, https://doi.org/10.1038/s41598-021-97118-5.

[14] M. Elgendi, "Fast QRS Detection with an Optimized Knowledge-Based Method: Evaluation on 11 Standard ECG Databases," *PLoS ONE*, vol. 8, no. 9, Sep. 2013, Art. no. e73557, https://doi.org/10.1371/journal.pone.0073557.

[15] M. Elgendi, M. Meo, and D. Abbott, "A Proof-of-Concept Study: Simple and Effective Detection of P and T Waves in Arrhythmic ECG Signals," *Bioengineering*, vol. 3, no. 4, Oct. 2016, Art. no. 26, https://doi.org/10.3390/bioengineering3040026.

[16] Q. Qin, J. Li, Y. Yue, and C. Liu, "An Adaptive and Time-Efficient ECG R-Peak Detection Algorithm," *Journal of Healthcare Engineering*, vol. 2017, pp. 1–14, 2017, https://doi.org/10.1155/2017/5980541.

[17] Q. Xiao *et al.*, "Deep Learning-Based ECG Arrhythmia Classification: A Systematic Review," *Applied Sciences*, vol. 13, no. 8, Apr. 2023, Art. no. 4964, https://doi.org/10.3390/app13084964.

[18] M. Hassaballah, Y. M. Wazery, I. E. Ibrahim, and A. Farag, "ECG Heartbeat Classification Using Machine Learning and Metaheuristic Optimization for Smart Healthcare Systems," *Bioengineering*, vol. 10, no. 4, Mar. 2023, Art. no. 429, https://doi.org/10.3390/bioengineering10040429.

[19] M. Kachuee, S. Fazeli, and M. Sarrafzadeh, "ECG Heartbeat Classification: A Deep Transferable Representation," in *2018 IEEE International Conference on Healthcare Informatics (ICHI)*, New York, NY, Jun. 2018, pp. 443–444, https://doi.org/10.1109/ICHI.2018.00092.

[20] M. Guanglong, W. Xiangqing, and Y. Junsheng, "ECG Signal Classification Algorithm Based on Fusion Features," *Journal of Physics: Conference Series*, vol. 1207, Apr. 2019, Art. no. 012003, https://doi.org/10.1088/1742-6596/1207/1/012003.

[21] T. Li and M. Zhou, "ECG Classification Using Wavelet Packet Entropy and Random Forests," *Entropy*, vol. 18, no. 8, Aug. 2016, Art. no. 285, https://doi.org/10.3390/e18080285.

[22] M. Tounsi, H. Ali, A. T. Azar, A. Al-Khayyat, and I. K. Ibraheem, "Comprehensive Learning Salp Swarm Algorithm with Ensemble Deep Learning-based ECG Signal Classification on Internet of Things Environment," *Engineering, Technology & Applied Science Research*, vol. 15, no. 1, pp. 19492–19500, Feb. 2025, https://doi.org/10.48084/etasr.8702.

[23] P. De Chazal, M. O'Dwyer, and R. B. Reilly, "Automatic Classification of Heartbeats Using ECG Morphology and Heartbeat Interval Features," *IEEE Transactions on Biomedical Engineering*, vol. 51, no. 7, pp. 1196–1206, Jul. 2004, https://doi.org/10.1109/TBME.2004.827359.

[24] W. Zhang, L. Yu, L. Ye, W. Zhuang, and F. Ma, "ECG Signal Classification with Deep Learning for Heart Disease Identification," in *2018 International Conference on Big Data and Artificial Intelligence (BDAI)*, Beijing, Jun. 2018, pp. 47–51, https://doi.org/10.1109/BDAI.2018.8546681.

[25] M. Wu, Y. Lu, W. Yang, and S. Y. Wong, "A Study on Arrhythmia via ECG Signal Classification Using the Convolutional Neural Network," *Frontiers in Computational Neuroscience*, vol. 14, Jan. 2021, Art. no. 564015, https://doi.org/10.3389/fncom.2020.564015.

[26] G. B. Moody and R. G. Mark, "The impact of the MIT-BIH Arrhythmia Database," *IEEE Engineering in Medicine and Biology Magazine*, vol. 20, no. 3, pp. 45–50, Jun. 2001, https://doi.org/10.1109/51.932724.

[27] *MIT-BIH Arrhythmia Database version 1.0.0.* (2005), G. Moody, R. Mark. [Online]. Available: https://physionet.org/content/mitdb/1.0.0/.

[28] S. Mallat, "Zero-crossings of a wavelet transform," *IEEE Transactions on Information Theory*, vol. 37, no. 4, pp. 1019–1033, Jul. 1991, https://doi.org/10.1109/18.86995.

[29] S. G. Mallat, "A theory for multiresolution signal decomposition: the wavelet representation," *IEEE Transactions on Pattern Analysis and Machine Intelligence*, vol. 11, no. 7, pp. 674–693, Jul. 1989, https://doi.org/10.1109/34.192463.

[30] C. Alvarado, J. Arregui, J. Ramos, and R. Pallas-Areny, "Automatic Detection of ECG Ventricular Activity Waves using Continuous Spline Wavelet Transform," in *2005 2nd International Conference on Electrical and Electronics Engineering*, Mexico City, Mexico, 2005, pp. 189–192, https://doi.org/10.1109/ICEEE.2005.1529605.

[31] E. Tsalera, A. Papadakis, and M. Samarakou, "Comparison of Pre-Trained CNNs for Audio Classification Using Transfer Learning," *Journal of Sensor and Actuator Networks*, vol. 10, no. 4, Dec. 2021, Art. no. 72, https://doi.org/10.3390/jsan10040072.

[32] G. Vega-Martinez, C. Alvarado-Serrano, and L. Leija-Salas, "ECG baseline drift removal using discrete wavelet transform," in *2011 8th International Conference on Electrical Engineering, Computing Science and Automatic Control*, Merida City, Mexico, Oct. 2011, pp. 1–5, https://doi.org/10.1109/ICEEE.2011.6106625.

[33] L. Moreno-Barón *et al.*, "Application of the wavelet transform coupled with artificial neural networks for quantification purposes in a voltammetric electronic tongue," *Sensors and Actuators B: Chemical*, vol. 113, no. 1, pp. 487–499, Jan. 2006, https://doi.org/10.1016/j.snb.2005.03.063.

AUTHORS PROFILE

Minh Phung is studying a B.S. degree in Electronics and Telecommunications Engineering at Ho Chi Minh City University of Technology (HCMUT). He can be contacted at: minh.phung2002sn@hcmut.edu.vn.

Hieu Nguyen received the B.S. degree in Control Engineering and Automation (2019) and the M.S. degree in Electronics Engineering (2021) from Ho Chi Minh City University of Technology (HCMUT), Vietnam. Currently, he is a PhD candidate in Electronics Engineering at HCMUT. He is also working as a lecturer at the Faculty of Electrical-Electronics Engineering, Ho Chi Minh City University of Technology – VNU HCM. He can be contacted at: hieunt@hcmut.edu.vn

Linh Tran received the B.S. degree in Electrical and Computer Engineering from the University of Illinois, Urbana–Champaign (2005), M.S. and PhD. in Computer Engineering from Portland State University (2006, 2015). Currently, he is working as lecturer at Faculty of Electrical-Electronics Engineering, Ho Chi Minh City University of Technology – VNU HCM. His research interests include quantum/reversible logic synthesis, computer architecture, hardware-software co-design, efficient algorithms and hardware design targeting FPGAs and deep learning. He can be contacted at: linhtran@hcmut.edu.vn.